Quantum Well Infrared Imaging Sensor with High-Sensitivity in the Wavelength Range of up to 15 µm

Daisuke KIMURA*, Sundararajan BALASEKARAN, Hiroshi INADA, Yasuhiro IGUCHI,
Michito SAKAI, and Masafumi KIMATA

Infrared detectors with Type-II superlattices are attracting increasing attention due to their theoretically higher performance and lower environment impact than HgCdTe detectors. While quite a number of reports have been made on sensor development, only a few of them have discussed a long wavelength region over 14 µm, which is required for hyper-spectral imaging. Using a Type-II InAs/GaInSb superlattice, we have developed an infrared imaging sensor (640 × 512, VGA format) that functions in the wavelength range of up to 15 µm. At a temperature of 77 K and a bias voltage of -20 mV, the sensor obtained a dark current density of 3.7×10^{-3} A/cm². The noise equivalent differential temperature (NEdT) of 0.29 K was achieved under an experimental condition using F/4 optics, a bias voltage of 0 mV, integration time of 200 µs, and temperature of 95 K. We succeeded in taking thermal images of a person.

Keywords: infrared imaging sensor, Type-II superlattice, VLWIR, VGA

1. Introduction

Infrared sensors that sensitively detect waves of 3 µm or longer have potential applications in toxic gas sensors, night-vision cameras, thermography, and environmental measurement of the Earth from space. Currently available infrared sensors mainly use HgCdTe as the photodetector material, however, it carries an environmental risk from its components, mercury and cadmium. To replace this material, InAs/GaSb Type-II superlattice, in which InAs and GaSb form a short-period sustained-layer, has become a focus of attention as a new environment-friendly photodetector material and is now being actively researched and developed. Figure 1 shows the band structure of InAs/GaSb superlattice. The InAs conduction band is lower than the GaSb valance band, and the miniband of an electron and miniband of a hole, which absorbs long-wavelength light, are formed. The InAs/GaSb superlattice has the following advantageous features compared with HgCdTe:

<1> It is theoretically predicted to lower the dark current as the Auger recombination can be suppressed due to the high effective mass of the carrier.

<2> Cutoff wavelength can be controlled between 3 µm and 30 µm by varying the thicknesses of the InAs and GaSb layers.

<3> Good uniformity is expected because III-V epitaxial growth techniques can be utilized.

Infrared sensors using an InAs/GaSb superlattice are actively being developed in the world, and a large number of research reports have been published concerning the medium wavelength infrared (MWIR, 3 to 5 µm wavelengths) region and the long wavelength infrared (LWIR, 8 to 14 µm wavelengths) region, which are atmospheric windows.[1]-[4] Further, detection in the very long wavelength infrared (VLWIR) region has a high potential of application in the area of hyperspectral imaging and remote sensing, where quantum features such as high sensitivity and fast response can be utilized.[5]-[7]
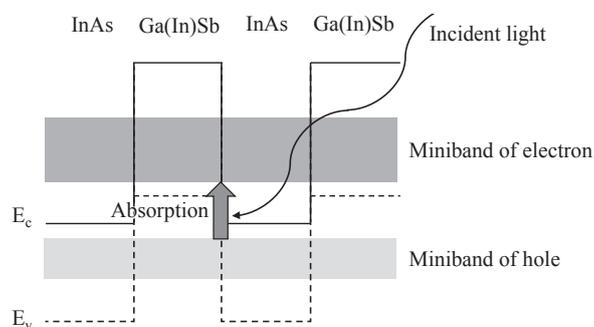

Fig. 1. Band structure of Type-II superlattice

This paper reports on our development of a 320,000-pixel infrared (IR) imaging sensor that functions in the wavelength range of up to 15 µm.

2. Device Structure

The structure of the epitaxial wafer is shown in Fig. 2.

For the absorption layer, we used an InAs/GaInSb superlattice. Compared to the InAs/GaSb superlattice, the InAs/GaInSb superlattice is expected to have high quantum efficiency and sensitivity, as the latter has a high absorption coefficient deriving from the large overlap of electron and hole wave functions.[6]

In order to reduce the dark current, we adopted a PbIbN structure, in which electron barrier and hole barrier layers are used on both sides of the absorption layer.[6],[8],[9]

Figure 3 represents the structure of the IR imaging sensor that we fabricated. The sensor has a mesa type structure, which is advantageous for high resolution imaging. The number of pixels was 320,000 [in a Video Graphics Array (VGA) format*1] with 15 µm pitch. The n-electrodes were formed on the InAsSb layer.
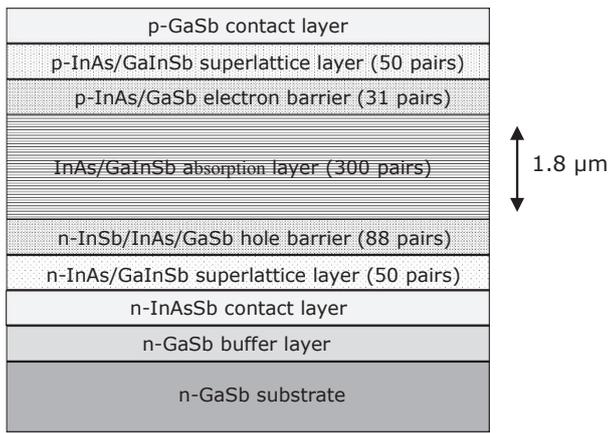
p-GaSb contact layer
p-InAs/GaInSb superlattice layer (50 pairs)
p-InAs/GaSb electron barrier (31 pairs)
InAs/GaInSb absorption layer (300 pairs)
n-InSb/InAs/GaSb hole barrier (88 pairs)
n-InAs/GaInSb superlattice layer (50 pairs)
n-InAsSb contact layer
n-GaSb buffer layer
n-GaSb substrate

1.8 μm

Fig. 2. Structure of epitaxial wafer

Fig. 3. Structure of IR imaging sensor

formed electrodes composed of the Ti/Pt/Au/Ni/Au layers through metal evaporation and the lift-off method. Next, we fabricated bumps made of In. The wafer was diced into sensor chips, and each chip and readout integrated circuit (ROIC)[*2] were connected via bumps using the flip-chip method. Underfill was injected into the gap between the chip and ROIC. Finally, the GaSb substrate was thinned down to 50 μm by chemical mechanical polishing (CMP) to reduce light absorbance.

1. Epitaxy growth
2. SiN film formation
3. Mask formation
4. Mesa formation
5. Passivation film formation
6. Electrode formation
7. In bump formation
8. Flip-chip bonding & underfill injection
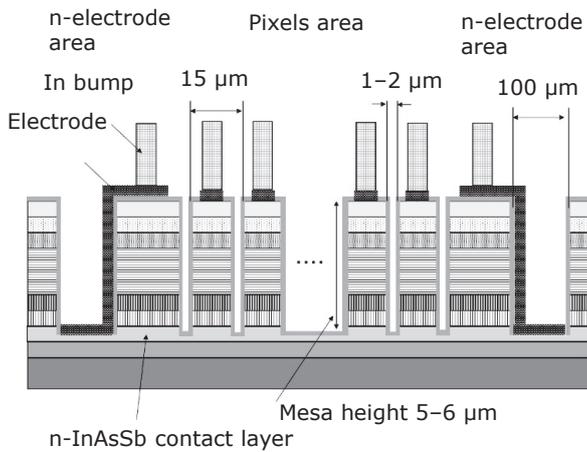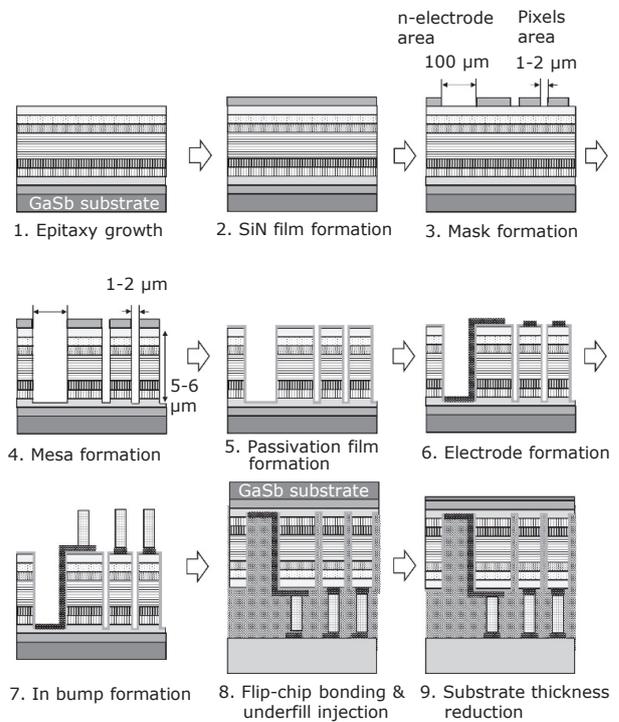9. Substrate thickness reduction

Fig. 4. Fabrication procedure of IR imaging sensor

3. Fabrication Process

Figure 4 summarizes the fabrication procedure of an IR imaging sensor. Layers were grown in the following order on the n-GaSb substrate using molecular beam epitaxy (MBE): n-GaSb buffer layer (0.5 μm thick), n-InAsSb contact layer (3 μm thick), n-InAs/GaInSb super-lattice layer (50 pairs), n-InSb/InAs/GaSb hole barrier layer (88 pairs), InAs/GaInSb absorption layer (300 pairs, 1.8 μm thick), p-InAs/GaSb electron barrier (31 pairs), p-InAs/GaInSb superlattice layer (50 pairs), and p-GaSb contact layer (0.2 μm thick). Next, SiN film was deposited on the p-GaSb contact layer and the IR imaging sensor pattern with 320,000 pixels (640 × 512 array) in 15 μm pitch was formed using photolithography. Next, SiN mask was formed and mesa formation was conducted by dry etching. The damaged layer at the side of the mesa was then removed by wet etching using a phosphate solution. Then, the SiN mask was removed using buffered hydrofluoric acid. In-situ N_2 plasma treatment was conducted to remove the native oxide from the surface, as well as to prevent re-oxidation. After the plasma treatment, an SiO_2 passivation film was deposited in the same chamber without breaking the vacuum.[10] We then opened contact holes and

Figure 5 shows an electron-microscope photograph of the IR imaging sensor that we fabricated. This reveals that mesas are laid out with an even and narrow pitch and have high aspect ratios.

Further, we fabricated a test element group with single photodiodes on the same wafer. This was used to estimate the IR imaging sensor characteristics, including the dark current and photodetector sensitivity.
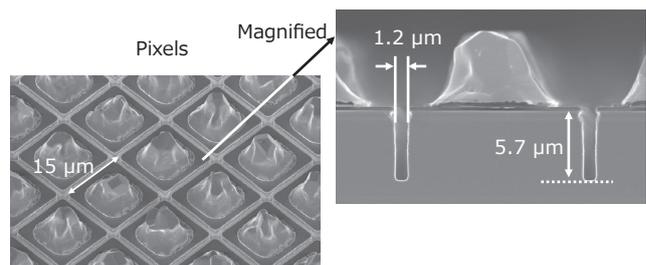
Fig. 5. Electron-microscope photograph of IR imaging sensor

4. Characteristics of IR Imaging Sensor

4-1 Characteristics of the dark current, spectral responsivity, and quantum efficiency

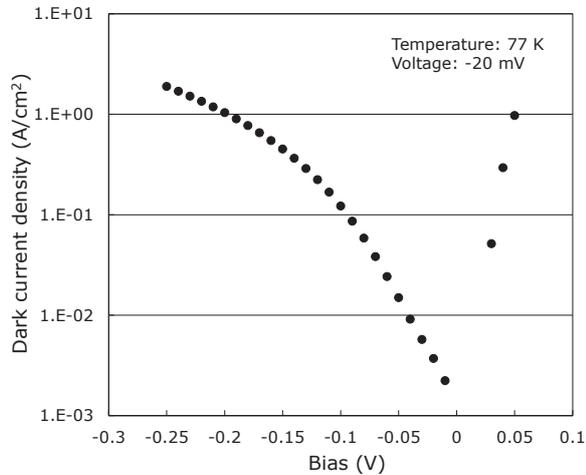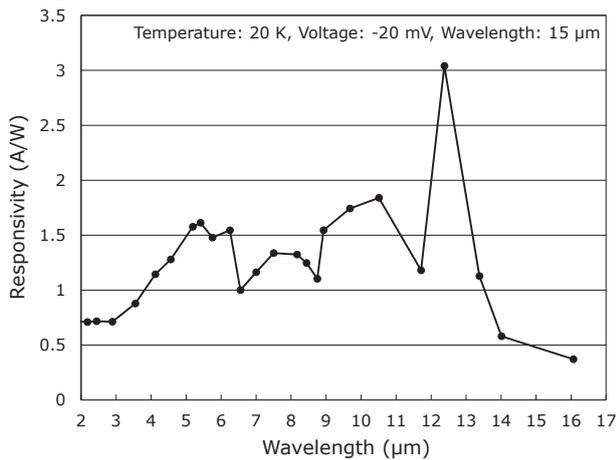The dark current, spectral responsivity, and quantum efficiency of the IR imaging sensor were measured using the single pixel sensor that was wire-bonded on the leadless chip carrier (LCC) package.
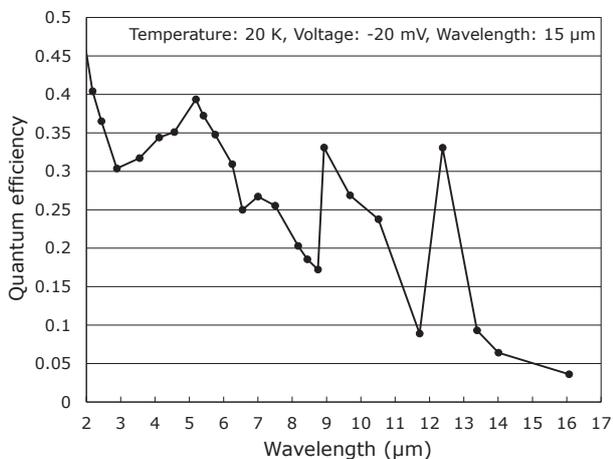
Dark current density is shown in Fig. 6, spectral responsivity in Fig. 7, and quantum efficiency in Fig. 8. (Note that the graphs in Figs. 7 and 8 are saw-toothed due to the interference of the peripheral effect.)

The dark current density at a temperature of 77 K and a voltage of -20 mV was 3.7×10^{-3} A/cm^2. The spectral responsivity at a temperature of 20 K, voltage of -20 mV, and wavelength of 15 μm was 0.5 A/W, and quantum efficiency was 5%.

4-2 Characteristics of imaging sensor

A thermal image of a person (Photo 1) was taken using the sensor chip cooled down to 94 K with liquid nitrogen, LWIR lens at f/1.4, integration time of 60 μs, and a 0 mV bias.

Also, a thermal image of a hand placed near the liquid nitrogen container was taken under the same conditions (Photo 2). As Photo 1 shows, the person's image was taken across the entire sensor. Photo 2 shows the gradation of the temperature difference of the hand and the liquid nitrogen container, which was cooler than room temperature.

Figure 9 is a histogram of noise equivalent differential temperature (NEdT) of the IR imaging sensor at a temperature of 95 K, an integration time of 200 μs, and a bias of 0 mV. The mode of NEdT was 0.29 K and operability at ±3σ was 85%.

Fig. 6. Dark current density

Fig. 7. Spectral responsivity

Fig. 8. Quantum efficiency

Photo 1. Thermal image of person

Photo 2. Thermal image of container cooled with liquid nitrogen

Fig. 9. Histogram of NEdT

References

(1) H. S. Kim, E. Plis, J. B. Rodriguez, G. D. Bishop, Y. D. Sharma, L. R. Dawson, S. Krishna, J. Bundas, R. Cook, D. Burrows, R. Dennis, K. Patnaude, A. Reisinger and M. Sundaram, Appl. Phys. Lett. 92 (2008) 183502

(2) V. Daumer, V. Gramich, R. Müller, J. Schmidt, F. Rutz, T. Stadelmann, A. Wörl and R. Rehm, Proc. of SPIE. (2017) 10177. 1017711

(3) L. Höglund, R. M. V. Würtemberg, C. Asplund, H. Kataria, A. Gamfeldt and E. Costard, Proc. of SPIE. (2017) 10177. 1017713.

(4) A. Rogalski, M. Kopytko and P. Martyniuk, Proc. of SPIE. (2017) 10177. 1017715

(5) Y. Wei, A. Gin and M. Razeghi, Appl. Phys. Lett. 81 (2002) 3675

(6) M. Sakai, J. Murooka, A. Kumeta, H. Katayama, T. Kimura, H. Inada, Y. Iguchi, Y. Hiroe and M. Kimata, Proc. of SPIE. (2016) 9933. 993306

(7) D. Jiang, W. Xiang, F. Guo, H. Hao, X. Han, X. Li, G. Wang, Y. Xu, Q. Yu, and Z. Niu, Appl. Phys. Lett. 108 (2016) 121110.

(8) N. Gautam, H. S. Kim, M. N. Kutty, E. Plis, L. R. Dawson and S. Krishna, Appl. Phys. Lett. 96 (2010) 231107

(9) P. Martyniuk, M. kopytko and A. Rogalski, Opto-Electron. Rev. 22 (2014) 127

(10) H. Inada, K. Machinaga, Sundararajan, B, K. Miura, Y. Tsuji, M. Migita, Y. Iguchi, H. Katayama and M. Kimata, Proc. of SPIE. (2014) 9070, 90700Z

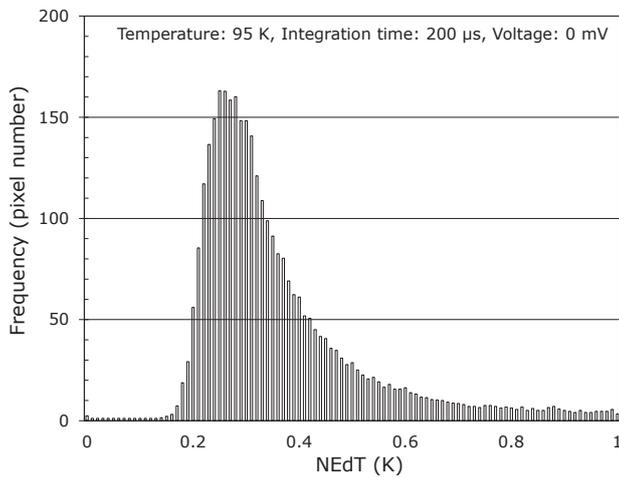## 5. Conclusion

Using a Type-II superlattice, we have developed an infrared imaging sensor (640 × 512, VGA format) that functions in the wavelength range of up to 15 μm. The sensor sensitivity was improved by adopting an InAs/ GaInSb superlattice as the absorption layer, and the dark current was reduced by having electron and hole barrier layers on both sides of the absorption layer. As a result, the noise equivalent differential temperature (NEdT) of 0.29 K was achieved and clear thermal images of a person were obtained. Although the uniformity of NEdT needs to be improved, the results were sufficiently significant to consider future applications in hyperspectral imaging and other purposes.

Technical Terms

∗1 Video Graphics Array (VGA): A format with 640 pixels horizontally and 512 pixels vertically.

∗2 Readout integrated circuit (ROIC): A circuit that retrieves electrical signals.

Contributors   The lead author is indicated by an asterisk (∗).

D. KIMURA∗
• Assistant Manager, Transmission Devices Laboratory

S. BALASEKARAN
• Ph.D.
 Assistant Manager, Transmission Devices Laboratory

H. INADA
• Group Manager, Transmission Devices Laboratory

Y. IGUCHI
• Dr. Eng.
 Department Manager, Transmission Devices Laboratory

M. SAKAI
• Ph.D.
 Japan Aerospace Exploration Agency (JAXA)

M. KIMATA
• Ph.D.
 Professor, Ritsumeikan University